Comparative Assessment of Feed-forward Schemes with NCTF for sway and trajectory control of a DPTOC

M.A. Ahmad, R.M.T. Raja Ismail, M.S. Ramli and N. Hambali

Faculty of Electrical and Electronics Engineering
Universiti Malaysia Pahang,
Pekan, 26600, Pahang, Malaysia

Email: {mashraf, rajamohd, syakirin, najidah}@ump.edu.my

Abstract - **This paper presents a comparative assessment of feed-forward schemes in hybrid control schemes for anti-swaying and trajectory tracking of a double-pendulum-type overhead crane (DPTOC) system. A nonlinear DPTOC system is considered and the dynamic model of the system is derived using the Euler-Lagrange formulation. To study the effectiveness of the controllers, initially nominal characteristics following trajectory following (NCTF) is developed for position control of cart movement. The controller design, which is comprised of a nominal characteristic trajectory (NCT) and PI compensator, is used to make the cart motion follow the NCT. This is then extended to incorporate feed-forward schemes for anti-swaying control of the system. Feed-forward control schemes based on input shaper and filtering techniques are to be examined. The input shaper and filtering techniques with different orders were designed based on properties of the system. The results of the response with the controllers are presented in time and frequency domains. The performances of hybrid control schemes are examined in terms of level of input tracking capability, sway angle reduction and time response specifications in comparison to NCTF controller. Finally, a comparative assessment of the control techniques is discussed and presented.**

Index Terms – Double-pendulum-type overhead crane, anti-sway control, NCTF control, input shaping, low pass filter.

I. INTRODUCTION

Various attempts in controlling cranes system based on open loop and closed-loop control system have been proposed. For example, open loop time optimal strategies were applied to the crane by many researchers [1,2]. Poor results were obtained in these studies because open-loop strategy is sensitive to the system parameters and could not compensate for the effect of wind disturbance. In other hand, feedback control which is well known to be less sensitive to disturbances and parameter variations has also been adopted for controlling the crane system. For example, PD controllers has been proposed for both position and anti-swing controls [3]. However, the performance of the controller is not very effective in eliminating the steady state error. In addition, an adaptive control strategy has also been proposed by Yang and Yang [4]. However, the control technique requires a nonlinear control theory which needs a complicated mathematical analysis. Besides, fuzzy logic controller has also been proposed for controlling the crane system by several researchers [3,5]. However, the fuzzy logic is still designed based on the model of the crane system.

In general, the above-mentioned control strategies would result in good performance when the exact model and its parameters are used in the design of the controller, which can only be done by an expert control engineer. In order to overcome these shortcomings, a nominal characteristic trajectory following (NCTF) control is introduced and examined in this paper. The NCTF with PI compensator proposed in this study is based on open-loop evaluation and without the need either to model crane or perform system identification. Originally, the NCTF controller is proposed as a practical controller for point-to-point (PTP) precision positioning system driven by an electric motor [6]. As the objective of the controlling crane system is to transfer a load from one location to another location, control of DPTOC system, therefore is identical to a PTP control system. However, the NCTF control is limited for position control of cart and cannot cater for sway control. To overcome this problem, a feed-forward scheme is incorporated to the system to suppress the sway of hook and load angle especially when the cart reaches the desired position [7]. The effectiveness of the proposed control method as well as the level of sway suppression is evaluated to a nonlinear DPTOC model.

The rest of this paper is structured in the following manner. The next section provides a brief description of the double pendulum-type overhead crane system considered in this study. Section 3 describes the modelling of the system derived using Euler-lagrange formulation whilst Section 4 describes the design of NCTF controller based on simple open loop evaluation. The design of input shaper and filtering schemes is explained in Section 5. Implementation results and comparative evaluation is reported in Section 6. Finally, concluding remarks are offered in the last section.

II. THE DOUBLE-PENDULUM-TYPE OVERHEAD CRANE SYSTEM

The DPTOC system with its hook and load considered in this work is shown in Figure 1, where x is the cart position, m is the cart mass, and m_1 and m_2 are the hook and load mass respectively. θ_1 is the hook swing angle, θ_2 is the load swing angle, l_1 and l_2 are the cable length of the hook and load, respectively, and F is the cart drive force. In

this simulation, the hook and load can be considered as point masses.

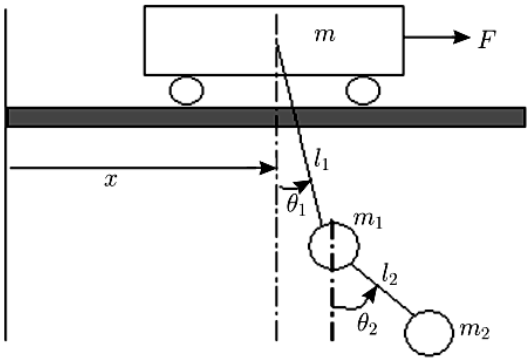

Figure 1 Description of the DPTOC system.

III. Dynamic Modeling of the Double-Pendulum-Type Overhead Crane

This section provides a brief description on the modeling of the DPTOC system, as a basis of a simulation environment for development and assessment of the hybrid control techniques. The Euler-Lagrange formulation is considered in characterizing the dynamic behavior of the crane system incorporate payload.

By Lagrange's equations, the dynamic model of the DPTOC system, shown in Figure 1, is assumed to have the following form [8]

$$M(q)\ddot{q} + C(q,\dot{q})\dot{q} + G(q) = \bar{\tau} \tag{1}$$

where the matrices $M(q) \in \Re^{3\times3}$, $C(q,\dot{q}) \in \Re^{3\times3}$, and $G(q) \in \Re^{3}$ represent the inertia, Centrifugal-Coriolis terms, and gravity, respectively, and are defined as

$$M(q) = \begin{bmatrix} m+m_1+m_2 & (m_1+m_2)l_1\cos\theta_1 & m_2 l_2\cos\theta_2 \\ (m_1+m_2)l_1\cos\theta_1 & (m_1+m_2)l_1^2 & m_2 l_1 l_2\cos(\theta_1-\theta_2) \\ m_2 l_2\cos\theta_2 & m_2 l_1 l_2\cos(\theta_1-\theta_2) & m_2 l_2^2 \end{bmatrix} \tag{2}$$

$$C(q,\dot{q}) = \begin{bmatrix} 0 & -(m_1+m_2)l_1\dot{\theta}_1\sin\theta_1 & -m_2 l_2\dot{\theta}_2\sin\theta_2 \\ 0 & 0 & m_2 l_1 l_2\dot{\theta}_1\sin(\theta_1-\theta_2) \\ 0 & -m_2 l_1 l_2\dot{\theta}_1\sin(\theta_1-\theta_2) & 0 \end{bmatrix} \tag{3}$$

$$G(q) = \begin{bmatrix} 0 & (m_1+m_2)gl_1\sin\theta_1 & m_2 g l_2\sin\theta_2 \end{bmatrix}^T \tag{4}$$

where g is the gravity effect. The state vector q and the control vector $\bar{\tau}$, are defined as

$$q = \begin{bmatrix} x & \theta_1 & \theta_2 \end{bmatrix}^T$$
$$\bar{\tau} = \begin{bmatrix} F & 0 & 0 \end{bmatrix}^T$$

After rearranging (1) and multiplying both sides by M^{-1}, one obtains

$$\ddot{q} = M^{-1}(-C\dot{q} - G + \bar{\tau}) \tag{5}$$

where M^{-1} is guaranteed to exist due to $\det(M) > 0$.

In this study the values of the parameters are defined as m=5 kg, m_1=2 kg, m_2=5 kg, l_1=2 m, l_2=1 m and g=9.8 m-s^{-2} [9].

IV. NCTF-PI Control Scheme

Figure 2 shows the structure of NCTF control system. The controller is composed of a nominal characteristic trajectory (NCT) and PI compensator. The objective of the PI compensator is to make the cart motion follow the NCT, finishing at the origin of the phase plane. The output of the NCT is a signal u_p, which is the difference between the actual error rate of the cart position ($-\dot{x}$) and the error rate of the NCT. On the phase-plane, the table motion is divided into a reaching phase and a following phase. During the reaching phase, the compensator controls the table motion to achieve the NCT. The next step is the following phase, where the PI compensator causes the cart motion to follow the NCT, leading it back to origin of the phase-plane.

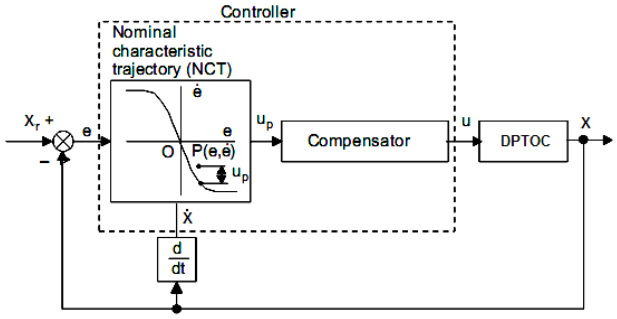

Figure 2 NCTF control structure.

The theoretical discussion and the previous NCT control design method is detailed in [10, 11]. The design of the NCTF controller comprised of three steps:

(i) The cart of the DPTOC is driven with an open-loop step input while its displacement and velocity are measured. Figure 3 shows the stepwise inputs, and the velocity and displacement responses due to the stepwise inputs. In this paper, the rated input to the

actuator u_r is used as the height of the stepwise inputs.

(ii) The NCT is constructed on the phase-plane using the displacement and velocity of the cart during the deceleration. From the curve in area *A* and *h* in Figure 3, the NCT in Figure 4 is determined. The inclination near origin, *m* and the maximum error rate, *h* relate with parameters of the plant as follows [10, 11]:

$$\beta = \frac{h}{u_r} \tag{6}$$

$$\alpha = -m \tag{7}$$

(iii) The PI compensator is designed using the open-loop response and the NCT information. The PI gains are chosen within the stable operation region which can be previously calculated independently of the actual crane characteristic. The proportional and integral compensator gains are calculated from

$$K_p = \frac{2\zeta\omega_n}{\alpha\beta} \tag{8}$$

$$K_i = \frac{{\omega_n}^2}{\alpha\beta} \tag{9}$$

where α and β are positive constants which relate to the plant dynamics. Meanwhile, ζ and ω_n are damping factor and natural frequency respectively. Here, ω_n and ζ are design parameters which should be decided by the designer. Most of the literatures prefer a larger value of ω_n and ζ in the design of PI compensator parameters. However, in this study, the value of ω_n and ζ are tuned using optimization toolbox in Matlab. With $\alpha = 4.9$ and $\beta = 1\times10^{-9}$, the optimum response of PI compensator is achieved by setting $K_p = 218.65$ and $K_i = 1\times10^{-4}$.

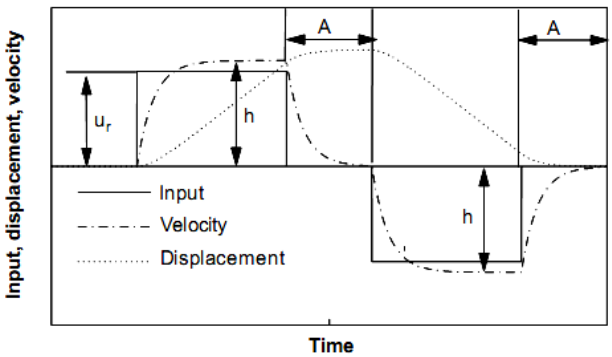

Figure 3 Stepwise inputs and responses.

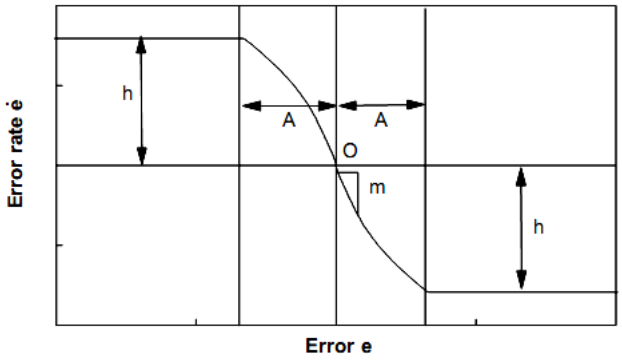

Figure 4 Nominal characteristics trajectory (NCT).

V. FEED-FORWARD CONTROL SCHEMES

A. *Input Shaper Control Schemes*

Input shaping technique is a feed-forward control technique that involves convolving a desired command with a sequence of impulses known as input shaper. The shaped command that results from the convolution is then used to drive the system. The input shaping process is illustrated in Figure 5. Design objectives are to determine the amplitude and time locations of the impulses, so that the shaped command reduces the detrimental effects of system flexibility. These parameters are obtained from the natural frequencies and damping ratios of the system. For the case of positive amplitudes, each individual impulse must be less than one to satisfy the unity magnitude constraint. The corresponding design relations for achieving a zero residual single-mode swaying of a system and to ensure that the shaped command input produces the same rigid body motion as the unshaped command yields a two-impulse sequence namely zero-swaying (ZS) with parameter as

$$t_1 = 0,\ t_2 = \frac{\pi}{\omega_d},\ A_1 = \frac{1}{1+K},\ A_2 = \frac{K}{1+K} \tag{10}$$

where

$$K = e^{-\zeta\pi/\sqrt{1-\zeta^2}},\quad \omega_d = \omega_n\sqrt{1-\zeta^2}$$

(ω_n and ζ representing the natural frequency and damping ratio respectively) and t_j and A_j are the time location and amplitude of impulse *j* respectively. In order to increase the robustness of the input shaper to errors in natural frequencies, the zero-sway-derivative-derivative (ZSDD) input shaper, is designed by solving the derivatives of the system vibration equation. This yields a four-impulse sequence with parameter as

$$t_1 = 0,\ t_2 = \frac{\pi}{\omega_d},\ t_3 = \frac{2\pi}{\omega_d},\ t_4 = \frac{3\pi}{\omega_d}$$

$$A_1 = \frac{1}{1+3K+3K^2+K^3},\ A_2 = \frac{3K}{1+3K+3K^2+K^3}$$

$$A_3 = \frac{3K^2}{1+3K+3K^2+K^3},\ A_4 = \frac{K^3}{1+3K+3K^2+K^3} \quad (11)$$

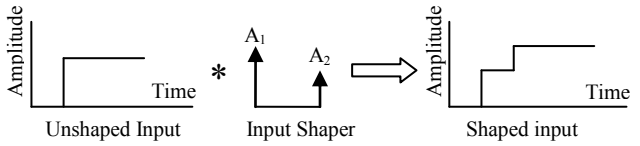

Figure 5 Illustration of input shaping technique.

B. Filtering Techniques

Filtering techniques is developed on the basis of extracting input energy around natural frequencies of the system. The filters are thus used for pre-processing the input signal so that no energy is fed into the system at the natural frequencies. In this manner, the flexural modes of the system are not excited, leading to a sway-free motion. This can be realised by employing either low-pass (LPF) or band-stop (BSF) filters. In the former, the filter is designed with a cut-off frequency lower than the first natural frequency of the system. In the latter case, band-stop filters with centre frequencies at the natural frequencies of the system are designed. This will require one filter for each mode of the system. The band-stop filters thus designed are then implemented in cascade to pre-process the input signal. There are various filter types such as Butterworth, Chebyshev and Elliptic that can be designed and employed. In this investigation, an infinite impulse response (IIR) Butterworth 3rd and 9th order low-pass filter are examined, respectively. In this study, low-pass filter with cut-off frequency at 50% of the first swaying mode were designed.

VI. Implementation and Results

In this investigation, hybrid control schemes for trajectory tracking and sway suppression are examined. Initially, a NCTF controller is designed to control the cart position. This is then extended to incorporate both input shaper (ZS and ZSDD) and low pass filter (3rd and 9th order) for control of sway of the system. The natural frequency was obtained by exciting the cart position with an unshaped reference input under NCTF controller. The feed-forward schemes were designed for pre-processing the trajectory reference input and applied to the system in a closed-loop configuration, as shown in Figure 6. In this study, the cart position of DPTOC is required to follow a unit step trajectory of 2 m. The responses of the DPTOC system to the unshaped trajectory reference input were analyzed in time-domain and frequency domain (spectral density). The first three modes of sway frequency of the system are considered, as these dominate the dynamic of the system. These results were considered as the system response to the unshaped input under tracking capability and will be used to evaluate the performance of the input shaping and filtering techniques.

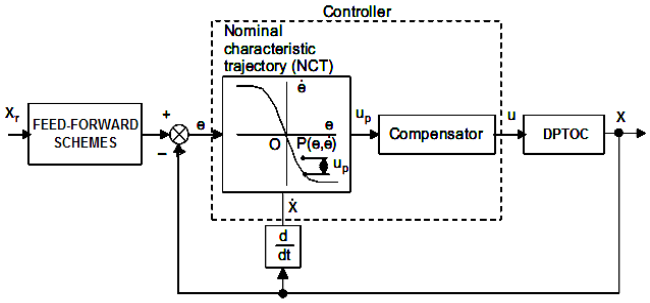

Figure 6 NCTF with feed-forward control structure.

Implementation results with NCTF controller have shown that the steady-state cart position trajectory of 2 m for the DPTOC system was achieved within the rise and settling times and overshoot of 0.507 s, 2.021 s and 2.1 % respectively. However, a noticeable amount of oscillation occurs during movement of the cart. It is noted from the sway of hook and load angle response with a maximum residual of ±0.8 rad and ±1.0 rad respectively. Moreover, from the PSD of both hook and load swing angle response, the sway frequency is dominated by the first three modes, which is obtained as 0.294 Hz, 0.883 Hz and 1.47 Hz. The closed loop parameters with the NCTF control will subsequently be used to design and evaluate the performance of hybrid controllers with input shaper and low pass filter.

In the case of input shaping control schemes, ZS and ZSDD shapers were designed for first three modes utilising the properties of the system. With the exact natural frequency of 0.294 Hz, 0.883 Hz and 1.47 Hz, the time locations and amplitudes of the impulses for both ZS and ZSDD shapers were obtained by solving equation (10) and (11) respectively. For digital implementation of the input shaping, locations of the impulses were selected at the nearest sampling time. However, in the case of low-pass filter, the input energy at all frequencies above the cut-off frequency can be attenuated. In this study, 3rd and 9th order low-pass filters with cut-off frequency at 50% of the first sway mode were designed. Thus, for the DPTOC system, the cut-off frequencies of the filters were selected at 0.147 Hz.

The corresponding rise time, settling time and overshoot of the cart position response and levels of sway attenuation for NCTF control with feed-forward control are depicted in Table 1. It is noted that the highest level of sway reduction were obtained using NCTF with ZSDD shaper and NCTF with 9th order LPF for hook and load sway angle respectively. The trend shows that the level of sway reduction increases with the increase in number of order and impulse sequence for LPF and input shaper respectively.

Table 1: Level of sway reduction of the hook and load swing angle and specifications of cart position response.

Feed-forward Schemes	Types of shaper	Swing angle	Attenuation (dB) of sway of the cable			Specification of cart position response		
			Mode 1	Mode 2	Mode 3	Rise time (s)	Settling time (s)	Overshoot (%)
Input Shaper	ZS	Hook swing angle, θ_1	27.22	53.42	32.11	2.406	2.977	0.05
		Load swing angle, θ_2	26.44	40.29	29.25			
	ZSDD	Hook swing angle, θ_1	40.39	85.83	81.64	4.229	7.201	0.00
		Load swing angle, θ_2	39.57	78.63	74.10			
Low pass filter	3rd order	Hook swing angle, θ_1	16.85	74.61	63.22	2.491	7.451	7.85
		Load swing angle, θ_2	17.13	71.61	76.76			
	9th order	Hook swing angle, θ_1	40.56	79.84	72.44	3.238	21.41	17.00
		Load swing angle, θ_2	41.26	88.43	79.12			

However, in terms of speed of response, NCTF with ZS shaper produce the fastest response followed by ZSDD shaper, 3rd order and 9th order LPF. It shows that the speed of the system response reduces with the increase in number of order and impulse sequence for both LPF and input shaper respectively. It is also noted that the differences in rise times of the cart position response for the hybrid control schemes are negligibly small. In overall, a slower cart position response for NCTF with feed-forward control schemes, as compared to the NCTF control, was achieved.

For comparative assessment, the levels of sway attenuation of the hook's and load's sway angle using the feed-forward schemes are shown with the bar graph in Figure 7 and 8 respectively. In overall, low pass filter techniques provide better performance in sway reduction as compared to input shaper especially for the second and third mode. The result also shows that the low pass filter techniques obtained higher level of sway attenuation at the load swing angle as compared to hook swing angle. This trend is slightly difference in input shaper results. Comparisons of the specifications of the cart position responses using the NCTF control with feed-forward are summarised in Figure 9 for the rise and settling times. It is noted that a slower cart position response for low pass filter techniques as compared to input shaper schemes. In addition, using the low pass filter technique, an unacceptable overshoot occurs during movement of the cart as compared to input shaper schemes. This is due to the effect of the low pass filter technique that results a high overshoot at the filtered input.

VII. CONCLUSION

The development of hybrid control schemes based on NCTF control with feed-forward schemes for input tracking and sway suppression of a DPTOC system has been presented. The performances of the control schemes have been evaluated in terms of input tracking capability, level of sway reduction and time response specifications. Acceptable performance in input tracking control and sway suppression has been achieved with both control strategies. Moreover, a significant reduction in the system sway has been achieved with the hybrid controllers regardless of the number of filter's orders and impulses in the low pass filter and input shaper design respectively. It is concluded that the proposed hybrid controllers are capable of reducing the system sway while maintaining the input tracking performance of the DPTOC.

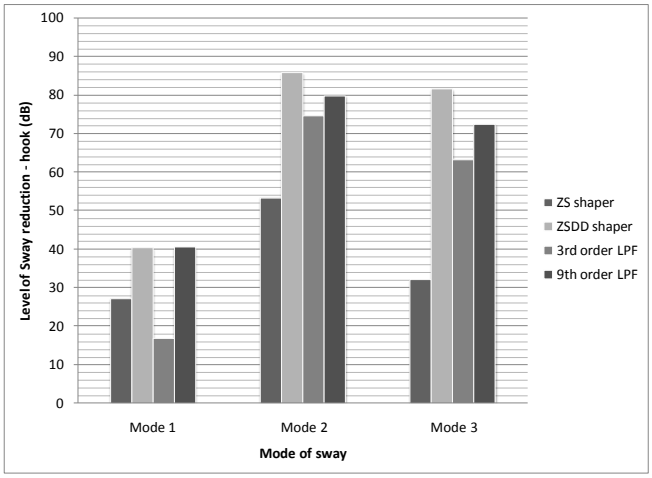

Figure 7 Level of sway (hook) reduction using NCTF with feed-forward control schemes.

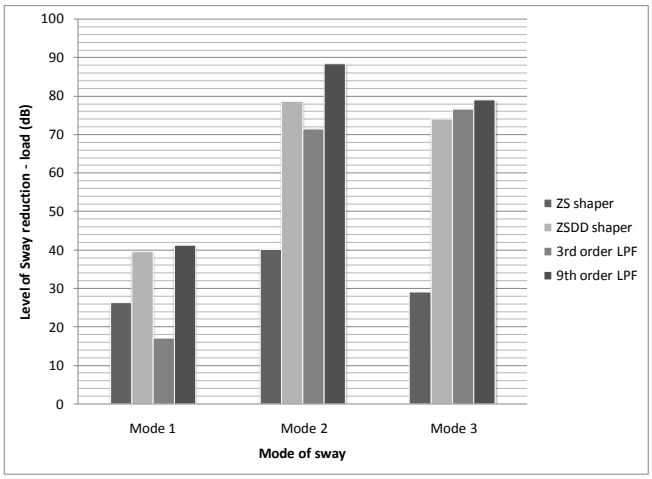

Figure 8 Level of sway (load) reduction using NCTF with feed-forward control schemes.

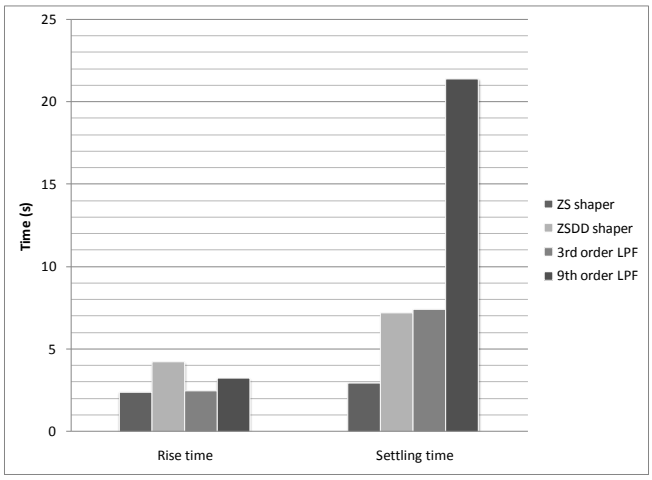

Figure 9 Rise and settling times of cart position response using NCTF with feed-forward control schemes.

ACKNOWLEDGMENT

This work was supported by Faculty of Electrical & Electronics Engineering, Universiti Malaysia Pahang, especially Control & Instrumentation (COINS) Research Group under research grant RDU090350.

REFERENCES

[1] G.A. Manson, "Time-Optimal Control of and Overhead Crane Model," *Optimal Control Applications & Methods*, 3(2), 1992, pp. 115-120.

[2] J. Auernig and H. Troger, "Time Optimal Control of Overhead Cranes with Hoisting of the Load," *Automatica*, 23(4), 1987, pp. 437-447.

[3] H.M. Omar, Control of Gantry and Tower Cranes, M.S. Thesis, Virginia Tech., 2003, Blacksburg, VA.

[4] J.H. Yang, and K.H. Yang, "Adaptive coupling control for overhead crane systems," Available from: http://www.sciencedirect.com, Accessed : 2006-12-24.

[5] H.H. Lee and S.K. Cho, "A New fuzzy logic anti-swing control for industrial three-dimensional overhead crane," *Proceedings of the 2001 IEEE International Conference on Robotic and Automation*, 2001, Seoul, pp. 2958-2961.

[6] Wahyudi, K. Sato and A. Shimokohbe, "Robustness Evaluation of New Practical Control Method for PTP Positioning Systems," *Proceedings of 2001 IEEE/ASME International Conference on Advanced Intelligent Mechatronics*, 2001, Como, Italy, pp. 843-848.

[7] M.A. Ahmad, R.M.T. Raja Ismail, M.S. Ramli, A.N.K. Nasir and N. Hambali, "Feed-forward Techniques for Sway Suppression in a Double-Pendulum-Type Overhead Crane," *Proceedings of International Conference on Computer Technology and Development*, 2009, K. Kinabalu, Malaysia, pp. 173-178.

[8] M.W. Spong, Underactuated Mechanical Systems, Control Problems in Robotics and Automation. London: Springer-Verlag, 1997.

[9] D.T. Liu, W.P. Guo and J.Q. Yi, "Dynamics and Stable Control for a Class of Underactuated Mechanical Systems," *Acta Automatica Sinica*, Vol. 32, No. 3, 2006, pp. 422-427.

[10] Wahyudi, K. Sato and A. Shimokohbe, "Characteristics of practical control for point-to-point (PTP) positioning systems effect of design parameters and actuator saturation on positioning performance," *Precision Engineering*, Vol. 27, 2003, pp. 157-169.

[11] K.Sato, K. Nakamoto and A. Shimokohbe, "Practical control of precision positioning mechanism with friction," *Precision Engineering*, Vol. 28, 2004, pp. 426-434.